

Thermal effects of the quantum states generated from the isomorphs of PPKTP crystal

Rui-Bo Jin^{1,2,*}, Guo-Qun Chen¹, Fabian Laudenbach^{3,4}, Shengmei Zhao², and Pei-Xiang Lu¹
¹Laboratory of Optical Information Technology, Wuhan Institute of Technology, Wuhan 430205, China

²Key Lab of Broadband Wireless Communication and Sensor Network Technology,
Nanjing University of Posts and Telecommunications, Ministry of Education

³Security & Communication Technologies, Center for Digital Safety & Security,
AIT Austrian Institute of Technology GmbH, Donau-City-Str. 1, 1220 Vienna, Austria and

⁴Quantum Optics, Quantum Nanophysics and Quantum Information,
Faculty of Physics, University of Vienna, Boltzmanngasse 5, 1090 Vienna, Austria

We theoretically and numerically investigate the temperature-dependent properties of the biphotons generated from four isomorphs of periodically poled KTiOPO_4 (PPKTP): i.e., PPRTP, PPKTA, PPRTA and PPCTA. It is discovered that the first type of group-velocity-matched (GVM) wavelength is decreased by 6.4, 1.2, 8.9, 25.6 and 6.3 nm, while the phase-matched wavelength is decreased by 4.4, -0.4, -1.2, 29.1 and 59.5 nm for PPKTP, PPRTP, PPKTA, PPRTA and PPCTA, respectively, when the temperature is increased from 20 °C to 120 °C. Although the maximal spectral purity of the heralded single photons is not changed at different temperature, the Hong-Ou-Mandel (HOM) interference shows different patterns due to a shift of the joint spectral amplitude. These thermal effects are very important for precise control of the quantum state for the future applications in quantum information processing, for example, in quantum interference or spectroscopy.

I. INTRODUCTION

Quantum state engineering using nonlinear optical crystals in a spontaneous parametric down-conversion (SPDC) process is a very important technique for the study of quantum information processing (QIP)[1, 2]. Periodically poled KTiOPO_4 (PPKTP) is one of the widely used crystals, because it satisfies the group-velocity-matched (GVM) condition and therefore can be used to prepare spectrally pure state at telecom wavelength [3–14]. Recently, it was discovered that spectrally pure states can also be generated from four isomorphs of the PPKTP, i.e., periodically poled RTP (RbTiOPO_4), KTA (KTiOAsO_4), RTA (RbTiOAsO_4) and CTA (CsTiOAsO_4), with a general form of $MTiOXO_4$ with $\{M = \text{K, Rb, Cs}\}$ and $\{X = \text{P, As (for } M=\text{Cs only)}\}$ [15–17]. It was found that these isomorphs still retain the desirable properties of their parent PPKTP, namely high spectral purity (over 0.8) with wide frequency tunability (more than 400 nm) at a variety of wavelengths (from 1300 nm to 2100 nm). These isomorphs may provide more and better choices for quantum state engineering at telecom wavelengths.

In the previous study in Refs. [15, 16], the properties of the quantum state generated from the $MTiOXO_4$ are investigated only at room temperature, i.e., 20 °C. However, their temperature-dependent properties are still unexplored. Temperature is an important parameter for these quasi-phase matched (QPM) crystals, because the phase-matching condition in the QPM crystals is mainly controlled by temperature in experiment. Temperature is also the key to precisely control the quantum state in

many QIP applications, e.g., in fine tuning of the quantum wave function [18] and entanglement [19], in spectroscopy [20] and quantum interference [21]. For future applications of these isomorphs, it is therefore very important and necessary to investigate the temperature-dependent properties of quantum states generated by these materials. With this motivation, in this work we study the thermal effect on spectrally-pure-state generated from the periodically poled $MTiOXO_4$ crystals.

This paper is organized as follows: Section I is the introduction part. In section II, we study the GVM wavelength of the five crystals as a function of temperature. In section III, the phase matched wavelength as a function of temperature will be explored. In section IV, we study the thermal effect on the joint spectral amplitude (JSA) of the biphotons generated from the isomorphs. Based on different JSAs, different Hong-Ou-Mandel (HOM) interference patterns are also investigated. Then, we provide some discussions in section V and summarize the paper in section VI.

II. THERMAL EFFECT ON THE GVM WAVELENGTH

The GVM wavelength is an important parameter for the nonlinear crystals since it is the wavelength at which maximal spectral purity can be achieved. There are three types of GVM conditions [2]:

$$2V_{g,p}^{-1}(\lambda/2) = V_{g,s}^{-1}(\lambda) + V_{g,i}^{-1}(\lambda), \quad (1)$$

$$V_{g,p}^{-1}(\lambda/2) = V_{g,s(i)}^{-1}(\lambda), \quad (2)$$

* jrbqyj@gmail.com

Name Composition	PPKTP KTiOPO ₄	PPRTP RbTiOPO ₄	PPKTA KTiOAsO ₄	PPRTA RbTiOAsO ₄	PPCTA CsTiOAsO ₄
λ_{GVM1} at 20 °C (nm)	1584.6	1643.2	1680.9	1786.6	1972.5
$\Delta\lambda_{GVM1}$ 20-120 °C (nm)	6.4	1.2	8.9	25.6	6.3
λ_{GVM2} at 20 °C (nm)	1225.2	1282.0	1288.1	1379.7	1577.2
$\Delta\lambda_{GVM2}$ 20-120 °C (nm)	7.3	-2.4	-2.1	22.4	5.4
$\Delta\lambda_{PM}$ 20-120 °C (nm)	4.4	-0.4	-1.2	29.1	59.5
References	[22–25]	[26–28]	[25, 29–31]	[17, 28, 32]	[33, 34]

TABLE I. Comparison of the chemical composition, λ_{GVM1} , $\Delta\lambda_{GVM1} = \lambda_{GVM1}(20^\circ\text{C}) - \lambda_{GVM1}(120^\circ\text{C})$, λ_{GVM1} , $\Delta\lambda_{GVM2} = \lambda_{GVM2}(20^\circ\text{C}) - \lambda_{GVM2}(120^\circ\text{C})$ and $\Delta\lambda_{PM}$ of PPKTP and four of its isomorphs. The relevant sources in the literatures for the appropriate Sellmeier the thermal-optical equations are also listed in the table.

and

$$V_{g,s}^{-1}(\lambda) = V_{g,i}^{-1}(\lambda), \quad (3)$$

where $V_{g,\mu}^{-1}(\mu = p, s, i)$ is the inverse of the group velocity $V_{g,\mu}$ for the pump p , the signal s , and the idler i . λ is the degenerate wavelength of the signal and idler. In our theoretical model, p , s and i propagate in a collinear configuration along the crystal's x axis. p and s polarize along the crystal's y axis, while i polarizes along the crystal's z axis. The group velocity can be calculated using the equation

$$V_{g,\mu} \equiv \frac{d\omega}{dk} = \frac{c}{n - \lambda dn}, \quad (4)$$

where c is the light velocity, ω is the angular frequency, k is the wave vector and n is the refractive index, which is a function of wavelength and temperature. Each of the three GVM conditions has special applications in quantum state engineering. For example, the first GVM wavelength (λ_{GVM1}) in Eq. (1) can be used to prepare a round-shape joint spectral distribution [3–7, 9–12, 23, 35]. The second GVM wavelength (λ_{GVM2}) in Eq. (2) can be used to prepare 90-degree-tilted oval-shape joint spectral distribution in KDP (KH₂PO₄) [36, 37]. The third GVM wavelength (λ_{GVM3}) in Eq. (3) can be used to prepare narrow, long and 45-degree-tilted JSA in a PPSLT (periodically poled MgO-doped stoichiometric LiTaO₃) crystal [38, 39]. In the case of $MTiOXO_4$ crystals, the third GVM condition can not be satisfied for type-II SPDC (although it can easily be satisfied for type-0 and type-I), therefore, we focus on the first two GVM conditions.

By using the Sellmeier equations and thermal-optical equations from the references as listed in Tab.I, we can calculate λ_{GVM1} and λ_{GVM2} . Fig.1(a1-e1) shows the λ_{GVM1} as a function of temperature from 20 °C to 120 °C. The λ_{GVM1} is decreasing when the temperature is increasing, as shown in Fig. 1. Different crystals exhibit different amounts of decrease, as listed in the insets of Fig. 1. With λ_{GVM1} shifting 25.6 nm, PPRTA has the biggest value of $\Delta\lambda$ while PPRTP shows the smallest wavelength shift of only 1.2 nm. Fig. 1(a2-e2) depicts λ_{GVM2} as a function of temperature. With increasing

temperature, λ_{GVM2} increases for PPRTP and PPKTA, while it decreases for the other crystals. PPRTA exhibits the biggest value of increase, i.e. 22.4 nm while PPKTA has the smallest value of 2.1 nm.

III. THERMAL EFFECT ON THE PHASE MATCHING WAVELENGTH

Another important parameter for SPDC is the phase matching wavelength, which can be obtained by solving the equation sets of

$$\frac{1}{\lambda_p} - \frac{1}{\lambda_s} - \frac{1}{\lambda_i} = 0, \quad (5)$$

and

$$k_p - k_s - k_i + \frac{2\pi}{\Lambda} = 0, \quad (6)$$

where Λ is the poling period. In fact, Eq. (5) corresponds to the energy conservation law and Eq. (6) corresponds to the momentum conservation law during the SPDC process.

Note, the GVM wavelength λ_{GVM} is different from the phase-matched wavelength λ_{PM} , and these two parameters are independent from each other. Generally speaking, λ_{PM} is the wavelength where SPDC occurs, while λ_{GVM} is the wavelength where pure quantum state can be engineered. λ_{PM} is determined by the zero-order dispersion ($n(\lambda)$) of the crystal, while λ_{GVM} is determined by the first order of dispersion ($\frac{dn(\lambda)}{d\lambda}$). At a fixed temperature, the λ_{GVM} is fixed, but the λ_{PM} can be shifted to any wavelength, as long as Eq. (5) and Eq. (6) are satisfied.

Figure 2(a-e) show the phase matched wavelength as a function of the temperature from 20 °C to 120 °C for the $MTiOXO_4$. Here, we set the pump wavelength at the half of λ_{GVM1} at 20 °C and keep the poling period Λ fixed. In Fig. 2, all the signal (red line) and idler (blue line) wavelength has a symmetric distribution around their GVM wavelength λ_{GVM1} . PPKTA shows a nonmonotonic change with the increase of temperature, while other crystals show a monotonic change. PPCTA

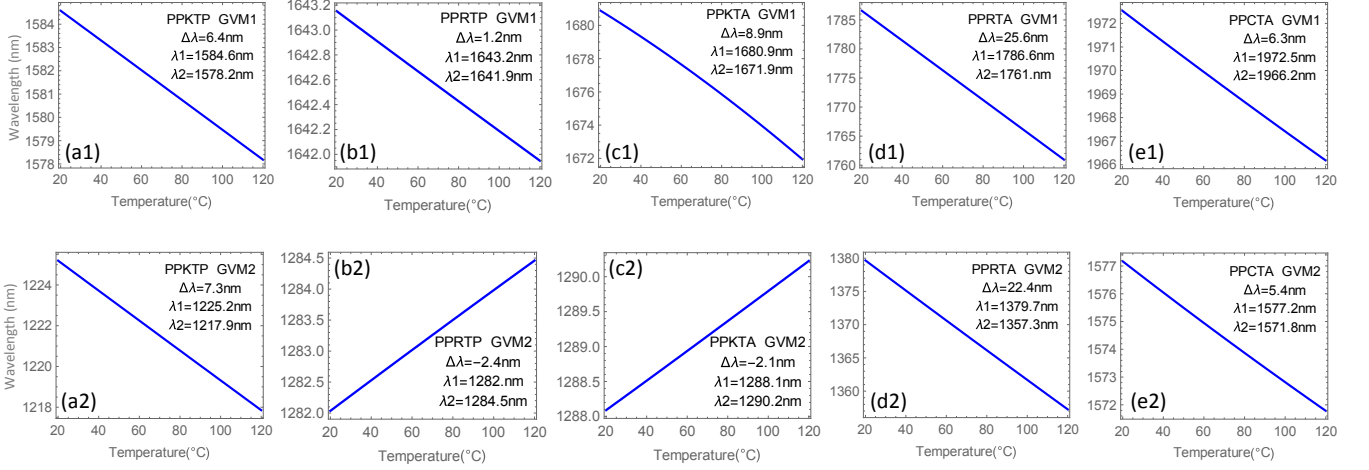


FIG. 1. λ_{GVM1} (first row) and λ_{GVM2} (second row) as a function of the temperature for different crystals. (a) PPKTP, (b) PPRTP, (c) PPKTA, (d) PPRTA and (e) PPCTA. Inset: $\lambda_{1(2)}$ is the wavelength at 20 (120) °C, and $\Delta\lambda = \lambda_1 - \lambda_2$.

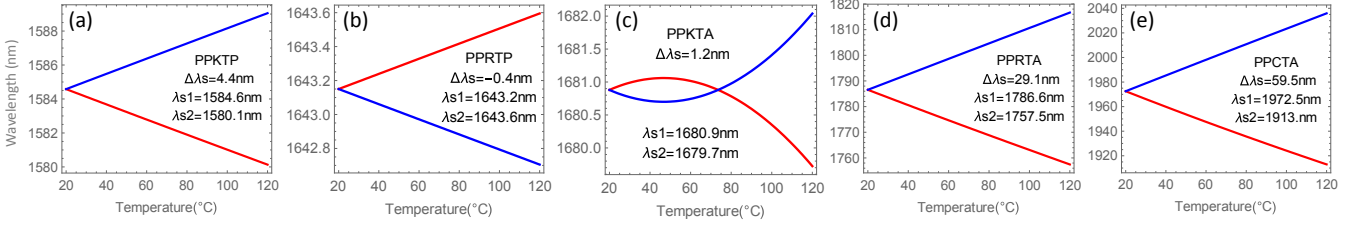


FIG. 2. The phase matched wavelength of signal (red line) and idler (blue line) as a function of temperature. (a) PPKTP, (b) PPRTP, (c) PPKTA, (d) PPRTA and (e) PPCTA. Inset: $\lambda_{s1(2)}$ is the wavelength of the signal at 20 (120) °C, and $\Delta\lambda_s = \lambda_{s1} - \lambda_{s2}$. In these plots, the poling period for each crystal is fixed to satisfy the degenerate type-II GVM1 condition at 20 °C.

is most sensitive to the temperature change. In contrast, PPRTP is very insensitive to temperature variance. With a temperature change from 20 °C to 120 °C, the wavelength is changed by 59.5 nm for PPCTA, while only 0.4 nm for PPRTP.

IV. THERMAL EFFECTS ON JOINT SPECTRAL DISTRIBUTION AND HONG-OU-MANDEL INTERFERENCE

With the Sellmeier and thermal-optical equation from the references as listed in Tab. I, we can also plot the joint spectral amplitude (JSA) as a function of temperature. The JSA can be calculated using the following equation

$$f(\omega_s, \omega_i) = \phi(\omega_s, \omega_i)\alpha(\omega_s + \omega_i) \quad (7)$$

where $\phi(\omega_s, \omega_i)$ and $\alpha(\omega_s + \omega_i)$ are the phase matching amplitude and the pump envelope amplitude. Assuming the pump spectrum has a Gaussian distribution with a bandwidth of σ_p , the pump envelope amplitude can be written as

$$\alpha(\omega_s + \omega_i) = \exp\left[-\left(\frac{\omega_s + \omega_i - \omega_p}{\sigma_p}\right)^2\right]. \quad (8)$$

Under the collinear configuration in the SPDC process, the phase matching amplitude can be written in the form of

$$\phi(\omega_s, \omega_i) = \text{sinc}\left(\frac{\Delta k L}{2}\right), \quad (9)$$

where $\Delta k = k_p - k_s - k_i + \frac{2\pi}{\Lambda}$, and L is the length of the SPDC crystal.

The change in the JSA has an immediate effect on the Hong-Ou-Mandel interference [40]. The two-fold coincidence probability in a HOM interference can be calculated using the following equation [41, 42].

$$p(\tau) = \frac{1}{4} \int_0^\infty \int_0^\infty d\omega_s d\omega_i \left| [f(\omega_s, \omega_i) - f(\omega_i, \omega_s) e^{-i(\omega_s - \omega_i)\tau}] \right|^2, \quad (10)$$

where τ is the time delay in the interference.

Each of the five crystals has different temperature-dependency in the HOM interference patterns. As an example, Fig. 3(a1-e1) shows the JSA of the signal and idler photons from PPCTA at the temperatures 20, 22, 25 and 30 °C. It can be observed that the JSA shifts to the top-left corner with the increase of the temperature. As a result, the frequency entanglement between

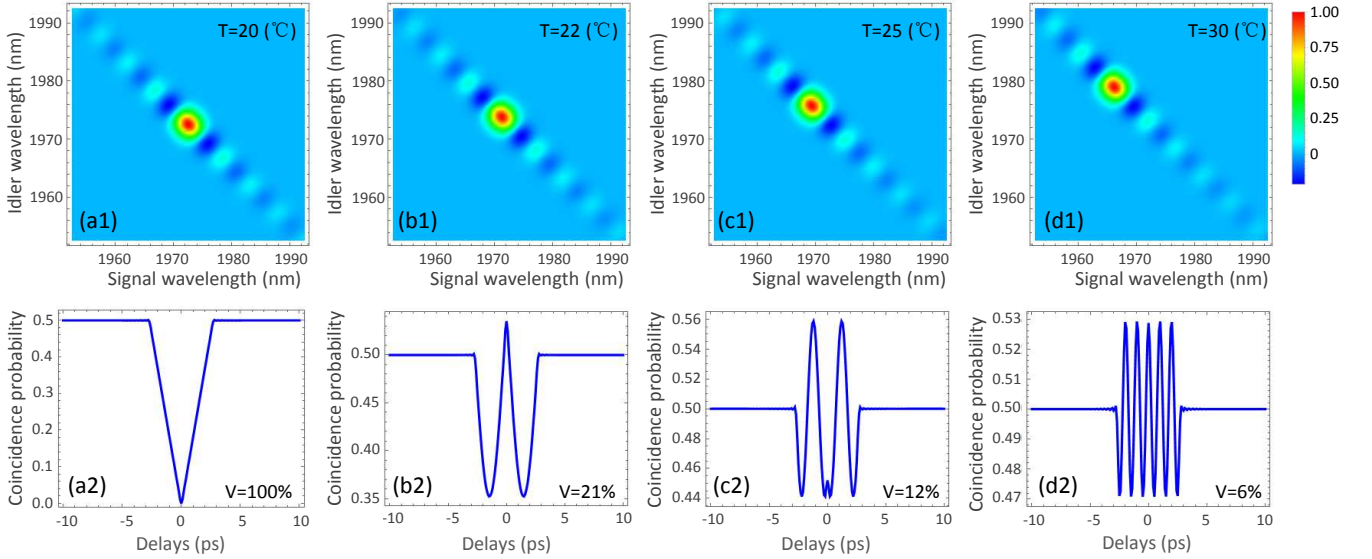


FIG. 3. The JSAs (first row) and HOM interference patterns (second row) at different temperatures: (a) 20 °C, (b) 22 °C, (c) 25 °C and (d) 30 °C. In this simulation, the PPCTA length is 30-mm-long, while the pump laser bandwidth (full-width-at-half-maximum) is 0.87 nm.

the signal and idler photons is shifted. Such a frequency shift doesn't change the purity of the biphoton source, but severely affects the HOM interference patterns, as shown in Fig. 3(a2-e2). By increasing the temperature from 20 to 22, 25 and 30 °C, the interference dips are changed from 1 to 2, 3, 6. The visibility, defined as $V = (P_{max} - P_{min}) / (P_{max} + P_{min})$, is decreased from 100% to 21%, 12% and 6%, where $P_{max(min)}$ is the maximal (minimal) value of $p(\tau)$.

V. DISCUSSION

It should be noticed that λ_{GVM1} varies slightly depending on the respective Sellmeier and thermal-optical equations measured by different groups, e.g., for PP-KTP at room temperature, $\lambda_{GVM1} = 1584.6$ nm and the poling period $\Lambda = 45.0$ μm can be calculated from Ref. [22], while $\lambda_{GVM1} = 1582.2$ nm and $\Lambda = 46.1$ μm can be obtained by using the Sellmeier equation of n_y from Ref. [23] and n_z from Ref. [24]. For PPKTA, $\lambda_{GVM1} = 1680.9$ and $\Lambda = 50.2$ μm can be calculated using Refs. [25, 29, 30], while $\lambda_{GVM1} = 1634.7$ and $\Lambda = 57.3$ μm with Ref. [31]. For PPRTA, $\lambda_{GVM1} = 1786.6$ and $\Lambda = 73.3$ μm can be calculated using Ref. [32], while $\lambda_{GVM1} = 1784.5$ and $\Lambda = 71.1$ μm with Ref. [17]. For PPCTA, $\lambda_{GVM1} = 1972.5$ and $\Lambda = 248.4$ μm can be calculated using Ref. [33], while $\lambda_{GVM1} = 1864.6$ and $\Lambda = 381.9$ μm with Ref. [17]. In the future, more experimental works are needed to obtain more accurate Sellmeier equations and thermal-optical equations for these crystals.

In Fig. 3, the visibility of the HOM interference was degraded at a higher temperature. In fact, the poling

period Λ of Eq. (6) is a design parameter that is available for tuning the phase matching condition. Therefore, by varying Λ appropriately for a specific temperature setting, the HOM visibility can be restored to unity by making sure that signal and idler wavelengths are the same.

The thermal-optical effect of quantum states generated from the isomorphs have many promising applications in the future. Firstly, temperature can be used for precise control of the spectral distribution of the quantum state. Sweeping the temperature can be used to scan the frequency. This is very useful for spectroscopy [20] or quantum interference [21]. Secondly, the crystals might be used for quantum sensing. PPCTA is very sensitive to temperature change, therefore it can be used as temperature sensor [43]. In contrast, PPRTP is very insensitive to temperature changes, therefore, this crystal can be used at different temperatures, as an anti-temperature-variance crystal.

The KTP family has 118 known isomorphs [44–46], with a general formula of $MM'OXO_4$, where $M = \text{K, Rb, Na, Cs, Tl, NH}_4$; $M' = \text{Ti, Sn, Sb, Zr, Ge, Al, Cr, Fe, V, Nb, Ta, Ga}$; $X = \text{P, As, Si, Ge}$. The Sellmeier equations and thermal-optical equation for most of these crystals are not reported yet, therefore, exploring the thermal optical properties of these crystal is promising for further research.

VI. CONCLUSION

In conclusion, we have theoretically and numerically investigated the temperature-dependent properties of biphoton states generated from the isomorphs of the PP-KTP crystal. Specifically, the first and second type of

GVM wavelength, the phase-matched wavelength, the JSA and HOM interference patterns as a function of temperature are explored in detail. It is found that different crystals have different thermal effects. We summarize the thermal-dependent properties of the crystals in Tab. I. The research results in this work should be very useful for the future applications, for example, in fine tuning of the spectrum in quantum interference or spectroscopy.

ACKNOWLEDGMENTS

This work is supported by the open research fund of Key Lab of Broadband Wireless Communication and Sensor Network Technology (Nanjing University of Posts and Telecommunications), Ministry of Education (Grant No. JZNY201709), by a fund from the Educational Department of Hubei Province, China (Grant No. D20161504), and by National Natural Science Foundations of China (Grant No. 61475075, 11104210 and 11704290).

-
- [1] W. P. Grice, A. B. U'Ren, and I. A. Walmsley, "Eliminating frequency and space-time correlations in multi-photon states," *Phys. Rev. A* **64**, 063815 (2001).
- [2] Keiichi Edamatsu, Ryosuke Shimizu, Wakana Ueno, Rui-Bo Jin, Fumihiko Kaneda, Masahiro Yabuno, Hirofumi Suzuki, Shigehiro Nagano, Atsushi Syouji, and Koji Suizu, "Photon pair sources with controlled frequency correlation," *Prog. Inform.* **8**, 19–26 (2011).
- [3] P. G. Evans, R. S. Bennink, W. P. Grice, T. S. Humble, and J. Schaake, "Bright source of spectrally uncorrelated polarization-entangled photons with nearly single-mode emission," *Phys. Rev. Lett.* **105**, 253601 (2010).
- [4] Thomas Gerrits, Martin J. Stevens, Burm Baek, Brice Calkins, Adriana Lita, Scott Glancy, Emanuel Knill, Sae Woo Nam, Richard P. Mirin, Robert H. Hadfield, Ryan S. Bennink, Warren P. Grice, Sander Dorenbos, Tony Zijlstra, Teun Klapwijk, and Val Zwiller, "Generation of degenerate, factorizable, pulsed squeezed light at telecom wavelengths," *Opt. Express* **19**, 24434–24447 (2011).
- [5] Andreas Eckstein, Andreas Christ, Peter J. Mosley, and Christine Silberhorn, "Highly efficient single-pass source of pulsed single-mode twin beams of light," *Phys. Rev. Lett.* **106**, 013603 (2011).
- [6] Rui-Bo Jin, Ryosuke Shimizu, Kentaro Wakui, Hugo Benichi, and Masahide Sasaki, "Widely tunable single photon source with high purity at telecom wavelength," *Opt. Express* **21**, 10659–10666 (2013).
- [7] Zhi-Yuan Zhou, Yun-Kun Jiang, Dong-Sheng Ding, and Bao-Sen Shi, "An ultra-broadband continuously-tunable polarization-entangled photon-pair source covering the C+L telecom bands based on a single type-II PPKTP crystal," *J. Mod. Opt.* **60**, 720–725 (2013).
- [8] Zhi-Yuan Zhou, Yun-Kun Jiang, Dong-Sheng Ding, Bao-Sen Shi, and Guang-Can Guo, "Actively switchable non-degenerate polarization-entangled photon-pair distribution in dense wave-division multiplexing," *Phys. Rev. A* **87**, 045806 (2013).
- [9] N. Bruno, A. Martin, T. Guerreiro, B. Sanguinetti, and R. T. Thew, "Pulsed source of spectrally uncorrelated and indistinguishable photons at telecom wavelengths," *Opt. Express* **22**, 17246–17253 (2014).
- [10] Yan Li, Zhi-Yuan Zhou, Dong-Sheng Ding, and Bao-Sen Shi, "CW-pumped telecom band polarization entangled photon pair generation in a Sagnac interferometer," *Opt. Express* **23**, 28792–28800 (2015).
- [11] Rui-Bo Jin, Mikio Fujiwara, Ryosuke Shimizu, Robert J. Collins, Gerald S. Buller, Taro Yamashita, Shigehito Miki, Hirofumi Terai, Masahiro Takeoka, and Masahide Sasaki, "Detection-dependent six-photon Holland-Burnett state interference," *Sci. Rep.* **6**, 36914 (2016).
- [12] Fabian Laudenbach, Hannes Hubel, Michael Hentschel, Philip Walther, and Andreas Poppe, "Modelling parametric down-conversion yielding spectrally pure photon pairs," *Opt. Express* **24**, 2712–2727 (2016).
- [13] Changchen Chen, Cao Bo, Murphy Yuezhen Niu, Feihu Xu, Zheshen Zhang, Jeffrey H. Shapiro, and Franco N. C. Wong, "Efficient generation and characterization of spectrally factorable biphotons," *Opt. Express* **25**, 7300–7312 (2017).
- [14] Rui-Bo Jin and Ryosuke Shimizu, "Extended Wiener-Khinchin theorem for quantum spectral analysis," *Optica* **5**, 93–98 (2018).
- [15] Rui-Bo Jin, Pei Zhao, Peigang Deng, and Qing-Lin Wu, "Spectrally pure states at telecommunications wavelengths from periodically poled MTiOXO₄ (M = K, Rb, Cs; X = P, As) crystals," *Phys. Rev. Appl.* **6**, 064017 (2016).
- [16] Fabian Laudenbach, Rui-Bo Jin, Chiara Greganti, Michael Hentschel, Philip Walther, and Hannes Hubel, "Numerical investigation of photon-pair generation in periodically poled MTiOXO₄ (M = K, Rb, Cs; X = P, As)," *Phys. Rev. Appl.* **8**, 024035 (2017).
- [17] L. K. Cheng, L. T. Cheng, J. Galperin, P. A. Morris Hotsenpiller, and J. D. Bierlein, "Crystal growth and characterization of KTiOPO₄ isomorphs from the self-fluxes," *J. Cryst. Growth* **137**, 107–115 (1994).
- [18] N. Tischler, A. Buse, L. G. Helt, M. L. Juan, N. Piro, J. Ghosh, M. J. Steel, and G. Molina-Terriza, "Measurement and shaping of biphoton spectral wave functions," *Phys. Rev. Lett.* **115**, 193602 (2015).
- [19] Alessandro Fedrizzi, Thomas Herbst, Markus Aspelmeyer, Marco Barbieri, Thomas Jennewein, and Anton Zeilinger, "Anti-symmetrization reveals hidden entanglement," *New J. Phys.* **11**, 103052 (2009).
- [20] R Whittaker, C Erven, A Neville, M Berry, J L OBrien, H Cable, and J C F Matthews, "Absorption spectroscopy at the ultimate quantum limit from single-photon states," *New J. Phys.* **19**, 023013 (2017).
- [21] Agata M. Brańczyk, Alessandro Fedrizzi, Thomas M. Stace, Tim C. Ralph, and Andrew G. White, "Engineered optical nonlinearity for quantum light sources,"

- Opt. Express **19**, 55–65 (2011).
- [22] Kiyoshi Kato and Eiko Takaoka, “Sellmeier and thermo-optic dispersion formulas for KTP,” Appl. Opt. **41**, 5040–5044 (2002).
- [23] Friedrich König and Franco N. C. Wong, “Extended phase matching of second-harmonic generation in periodically poled KTiOPO_4 with zero group-velocity mismatch,” Appl. Phys. Lett. **84**, 1644 (2004).
- [24] K. Fradkin, A. Arie, A. Skliar, and G. Rosenman, “Tunable midinfrared source by difference frequency generation in bulk periodically poled KTiOPO_4 ,” Appl. Phys. Lett. **74**, 914–916 (1999).
- [25] Shai Emanuel and Ady Arie, “Temperature-dependent dispersion equations for KTiOPO_4 and KTiOAsO_4 ,” Appl. Opt. **42**, 6661–6665 (2003).
- [26] Takuya Mikami, Takayuki Okamoto, and Kiyoshi Kato, “Sellmeier and thermo-optic dispersion formulas for RbTiOPO_4 ,” Opt. Mater. **31**, 1628–1630 (2009).
- [27] Jacques Mangin, Gabriel Mennerat, and Philippe Villerval, “Thermal expansion, normalized thermo-optic coefficients, and condition for second harmonic generation of a Nd:YAG laser with wide temperature bandwidth in RbTiOPO_4 ,” J. Opt. Soc. Am. B **28**, 873–881 (2011).
- [28] I. Yutis, B. Kirshner, and A. Arie, “Temperature-dependent dispersion relations for RbTiOPO_4 and RbTiOAsO_4 ,” Appl. Phys. B **79**, 77–81 (2004).
- [29] K. Fradkin-Kashi, A. Arie, P. Urenski, and G. Rosenman, “Mid-infrared difference-frequency generation in periodically poled KTiOAsO_4 and application to gas sensing,” Opt. Lett. **25**, 743–745 (2000).
- [30] D. L. Fenimore, K. L. Schepler, U. B. Ramabadran, and S. R. McPherson, “Infrared corrected Sellmeier coefficients for potassium titanyl arsenate,” J. Opt. Soc. Am. B **12**, 794–796 (1995).
- [31] K. Kato, “Second-harmonic and sum-frequency generation in KTiOAsO_4 ,” IEEE J. Quantum Electron. **30**, 881–883 (1994).
- [32] Kiyoshi Kato, Eiko Takaoka, and Nobuhiro Umemura, “Thermo-optic dispersion formula for RbTiOAsO_4 ,” Jpn. J. Appl. Phys. **42**, 6420 (2003).
- [33] Takuya Mikami, Takayuki Okamoto, and Kiyoshi Kato, “Sellmeier and thermo-optic dispersion formulas for CsTiOAsO_4 ,” J. Appl. Phys. **109**, 023108 (2011).
- [34] L. T. Cheng, L. K. Cheng, J. D. Bierlein, and F. C. Zumsteg, “Nonlinear optical and electro-optical properties of single crystal CsTiOAsO_4 ,” Appl. Phys. Lett. **63**, 2618–2620 (1993).
- [35] Rui-Bo Jin, Guo-Qun Chen, Hui Jing, Changliang Ren, Pei Zhao, Ryosuke Shimizu, and Pei-Xiang Lu, “Monotonic quantum-to-classical transition enabled by positively correlated biphotons,” Phys. Rev. A **95**, 062341 (2017).
- [36] Peter J. Mosley, Jeff S. Lundeen, Brian J. Smith, Piotr Wasylczyk, Alfred B. U’Ren, Christine Silberhorn, and Ian A. Walmsley, “Heralded generation of ultrafast single photons in pure quantum states,” Phys. Rev. Lett. **100**, 133601 (2008).
- [37] Rui-Bo Jin, Jun Zhang, Ryosuke Shimizu, Nobuyuki Matsuda, Yasuyoshi Mitsumori, Hideo Kosaka, and Keiichi Edamatsu, “High-visibility nonclassical interference between intrinsically pure heralded single photons and photons from a weak coherent field,” Phys. Rev. A **83**, 031805 (2011).
- [38] Ryosuke Shimizu and Keiichi Edamatsu, “High-flux and broadband biphoton sources with controlled frequency entanglement,” Opt. Express **17**, 16385–16393 (2009).
- [39] Rui-Bo Jin, Ryosuke Shimizu, Mikio Fujiwara, Masahiro Takeoka, Ryota Wakabayashi, Taro Yamashita, Shigehito Miki, Hiroataka Terai, Thomas Gerrits, and Masahide Sasaki, “Simple method of generating and distributing frequency-entangled qudits,” Quantum Sci. Technol. **1**, 015004 (2016).
- [40] C. K. Hong, Z. Y. Ou, and L. Mandel, “Measurement of subpicosecond time intervals between two photons by interference,” Phys. Rev. Lett. **59**, 2044–2046 (1987).
- [41] Rui-Bo Jin, Thomas Gerrits, Mikio Fujiwara, Ryota Wakabayashi, Taro Yamashita, Shigehito Miki, Hiroataka Terai, Ryosuke Shimizu, Masahiro Takeoka, and Masahide Sasaki, “Spectrally resolved Hong-Ou-Mandel interference between independent photon sources,” Opt. Express **23**, 28836–28848 (2015).
- [42] T. Gerrits, F. Marsili, V. B. Verma, L. K. Shalm, M. Shaw, R. P. Mirin, and S. W. Nam, “Spectral correlation measurements at the Hong-Ou-Mandel interference dip,” Phys. Rev. A **91**, 013830 (2015).
- [43] Sahar Basiri-Esfahani, Casey R. Myers, Ardan Armin, Joshua Combes, and Gerard J. Milburn, “Integrated quantum photonic sensor based on Hong-Ou-Mandel interference,” Opt. Express **23**, 16008–16023 (2015).
- [44] Anastasia P. Gazhulina and Mikhail O. Marychev, “Pseudosymmetric features and nonlinear optical properties of potassium titanyl phosphate crystals,” Cryst. Struct. Theory App. **2**, 106–119 (2013).
- [45] N. I. Sorokina and V. I. Voronkova, “Structure and properties of crystals in the potassium titanyl phosphate family: A review,” Crystallogr. Rep. **52**, 80–93 (2007).
- [46] Galen D. Stucky, Mark L. F. Phillips, and Thurman E. Gier, “The potassium titanyl phosphate structure field: a model for new nonlinear optical materials,” Chem. Mater. **1**, 492–509 (1989).